Sheet flow layer structure under oscillatory flows

P. A. Silva
CESAM & Departamento de Física, Universidade de Aveiro, Aveiro, Portugal

T. Abreu
Instituto Politécnico de Viseu, Viseu, Portugal

H. Michallet & D. Hurther
LEGI, Grenoble, France

F. Sancho
LNEC, Laboratório Nacional de Engenharia Civil, Lisboa, Portugal

ABSTRACT: Under large near-bed oscillatory velocities, sediment transport mainly occurs within a thin layer, known as the sheet flow layer. The structure of the sheet flow layer changes along the wave cycle, with maximum thickness around maximum onshore and off-shore velocities and minima at flow reversals. These changes are intimately related to the lower and upper bounds of the sheet flow layer. In the present work, the intra-wave changes of the sheet flow thickness for oscillatory flows, with acceleration and velocity skewnesses, are analysed based on detailed measurements of the sediment concentration within the bed layer and the backscattered signal of an Acoustic Doppler Velocity Profiler, located above. The results from both measurements are compared and discussed as a function of the physical forcing parameters: net current, flow acceleration and velocity skewnesses.

1 INTRODUCTION

Intense wave orbital velocities near the bed, occurring typically in the ocean surf zone or even at intermediate water depths during storm conditions, can cause the sand bed to move in as a sheet layer. This defines the so-called sheet flow layer (SFL), with thickness of the order of mm to cm, and sand concentrations reaching values between 200g/l to near 1600 g/l at the stationary bed. Due to the high concentration values, intergranular forces and sediment-flow forces are important. As shown by the experimental works of Ribberink and Al-Salem (1995) and McLean *et al*. (2001), most part of the sediment transport in this regime can occur in the SFL. Hence the study of the SFL structure along the wave cycle is an important research issue (Dohmen-Jansen, 1999; O'Donoghue and Wright, 2004; Hsu and Hanes, 2004; Myrhaug and Holmedal, 2007).

The sheet flow layer is divided into two distinct layers: a lower layer where the sediment particles are picked up from the bed and an upper layer in which they are entrained into the flow (see Figure 1). The boundary between the SFL and the upper suspension layer usually delimits two flow regions with distinct driving forces for the sediment movement: turbulent mixing in the suspension layer and intergranular forces in the SFL. As for volumetric concentrations higher than 0.08 (210 g/l) the intergranular forces are expected to be important, then the top of the SFL, d_t, is defined at this level (Dohmen-Janssen and Hanes, 2002).

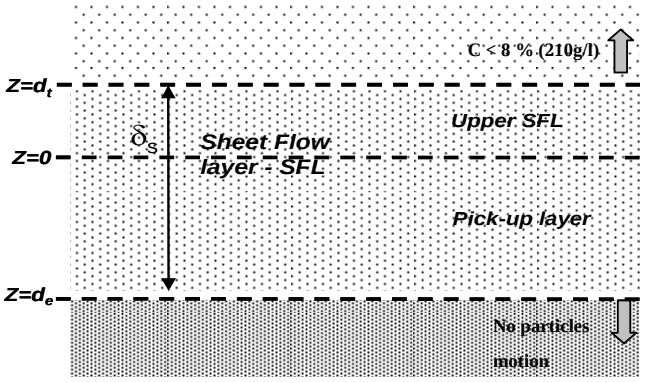

Figure 1. Diagram illustrating the sheet flow layer structure.

The lower level of the SFL, d_e, is considered as the instantaneous location of the interface between the moving and stationary grains. The difference between this level and the initial stationary bed, prior to wave motion, is considered by some authors as the erosion depth (e.g., Zala-Flores and Sleath, 1998). The boundary between the pick-up layer and the upper part of the SFL is normally found at z=0, the initial stationary bed. Following Dohmen-Janssen and Hanes (2002) and Ribberink *et al*. (2007), the SFL thickness is therefore defined as the distance between the top and lower levels, given above: $\delta_s = d_t - |d_e|$.

Due to the extremely challenging flow conditions, very few measurements exist so far across the SFL and the suspension layer. In the present work, we describe the sheet flow layer structure under acceleration- and velocity- skewed oscillatory flows with

and without opposing currents. The experimental data have been collected during a recent experimental project performed at the Large Oscillating Water Tunnel of Delft Hydraulics (Silva *et al*., 2008). These data consist of detailed measurements of sediment concentrations with two CCM probes (Conductivity Concentration Meter) and a high resolution ADVP (Acoustic Doppler Velocity Profiler). The backscattered acoustic intensity of the ADVP is processed for the determination of the SFL thickness along the wave cycle.

The SFL thickness obtained from the CCM and ADVP probes are compared and discussed as a function of the physical forcing parameters (net current, flow acceleration and velocity skewnesses).

2 EXPERIMENTAL SETUP

2.1 *LOWT and Instruments*

The experiments were performed in the Large Oscillating Water Tunnel (LOWT) at WL|Delft Hydraulics, the Netherlands, during the last trimester of 2007 (Silva *et al*., 2008). The experimental facility consists of a U-tube construction with a rectangular horizontal test section (14 m long, 0.3 m wide and 1.1 m height with a 0.3 m thick sand bed) and two cylindrical risers at either end. A piston system housed in one of the cylinders is capable to simulate near bottom horizontal velocities in the test section that correspond to full-scale wave conditions in the near shore-zone. The LOWT is fitted with a recirculation system that enables the generation of a mean current that can be superimposed on the oscillatory flow (see Ribberink and Al-Salem, 1994, for details).

The experiments were divided in two phases: the first part (M1) consisted of net sand transport rates measurements (Silva *et al*., 2008; Abreu *et al*., 2008); the second part (M2) consisted of detailed measurements of time-dependent sand concentrations and flow velocities in the suspension and sheet flow layers. In the present paper, we focus on the M2 measurements obtained with two conductivity concentration meters (CCM) and an Acoustic Doppler Velocity Profiler (ADVP).

The CCM (see Figure 2) has four-point electro-resistance probes. It measures the conductivity change of a sand-water mixture due to the variation of the quantity of sand particles present in the measuring volume (Ribberink and Al-Salem, 1995). The CCM were installed in the test section of the tunnel from bellow and can be displaced upwards and downwards within the sand bed and the water above.

The ADVP (see Figure 3) is under development at LEGI (Hurther *et al*., 2007; Mignot *et al*., 2009). It is composed of a sensor emitting at 2 MHz and two receivers positioned at the same depth (in this experiment about 35 cm above the bed) and 7.9 cm to the centre of the emitter. The acoustic pulse is repeated at 1.6 kHz. The backscattered acoustic signal is recorded every 4 μs. This enables to deduce velocities along the receivers beam axis over a whole profile with a vertical resolution of about 3 mm. Horizontal and vertical velocities are geometrically reconstructed from these components. 32 successive phase shifts are used to derive one value of the velocity. This leads to an equivalent acquisition frequency of 50 Hz. Velocity measurements are not presented in this paper. The analysis of the intensity of the received acoustic signal enables the estimation of the SFL boundary evolution with time.

The free stream velocity was measured with an Electromagnetic Flow Meter (EMF) placed above the wave boundary layer (z = 30 cm above the initial still bed level).

Figure 2. CCM probes.

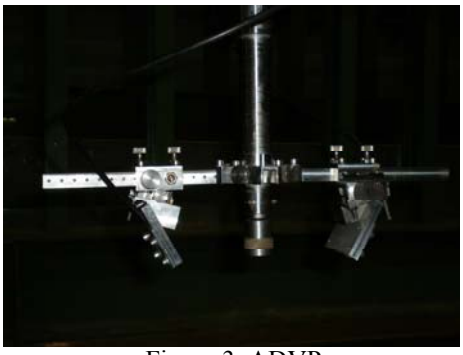

Figure 3. ADVP

Table 1. Experimental conditions

Condition	β (-)	R (-)	U_0 (m/s)
A1	0.65	0.5	0.0
A3	0.75	0.5	0.0
B2	0.65	0.5	-0.4
B4	0.75	0.5	-0.4
C1	0.50	0.6	0.0

2.2 *Test conditions*

The hydraulic conditions in the LOWT test section consisted of a repetition of regular oscillatory flows for the following three wave/current conditions: series A consisted of regular oscillatory flows with different degrees of acceleration skewness, $\beta = a_{\max}/(a_{\max} - a_{\min})$, where a is the acceleration; series B considered acceleration-skewed oscillatory flows with a collinear net current (U_0), opposing the wave direction; and series C considered both velocity and acceleration skewed oscillatory flows. The velocity skewness is characterized by

$R = u_{max}/(u_{max} - u_{min})$, where u is the flow velocity. The conditions for the 5 tests A1, A3, B2, B4 and C1 performed in M2 measurements are summarized in Table 1. The root-mean-square-value of the oscillatory velocity, u_{rms}, was maintained constant for all the conditions (~0.89 m/s) as well as the wave period (T=7s).

The experiments were performed with a well-sorted sand of median grain size d_{50} equal to 0.20 mm, placed in a 30 cm thick bed.

3 METHODOLOGY

The top and the lower level of the sheet flow layer during the oscillatory motion were established based on CCM and ADVP data and according to certain criterions that are described in the following. Analyses of video images collected during the experiments were also performed and enable to estimate the erosion depth.

3.1 *CCM*

The intra-wave lower level of the SFL, d_e, was computed by identifying the levels where the measured sediment concentration C did not change in time. As an example, Figure 4 represents the time-dependent phase-averaged concentration measured by the CCM for test B2 at different levels in the SFL.

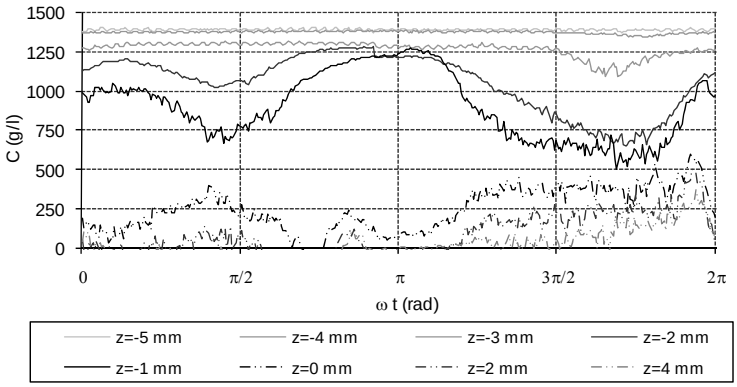

Figure 4. Time dependent phase-average sediment concentration measured by the CCM at different levels within the sheet flow layer (B2 test)

During the oscillatory motion, the concentration at z=–5 mm did not change and is equal to the still bed value. In the immediately upper level (z=–4 mm) the C values did change slightly in time for a small duration, during the wave trough. Therefore, during this time interval, the lower limit of the SFL is estimated at this level (i.e. d_e = –4 mm) with an accuracy of about 1 mm.

Small variations in the C measured values (10 - 20 g/l) were discarded in the computations of d_e. Instantaneous values of C above 8% vol. (approximately 210 g/l) define the upper limit of the SFL, d_t.

A linear interpolation was applied to compute d_t and d_e from the discrete levels where values of C were known. In most cases, the levels are located 1 mm apart; the accuracy in the d_t and d_e estimations is consequently of about 1 mm. The corresponding accuracy on the estimation of the SFL thickness δ_s is approximately 2 mm. Note that, according to Dohmen-Janssen and Hanes (2002), as the sampling volume of the CCM probes has a height of 1-1.5 mm, the values of SFL thickness less than 1.5 mm are not very accurate.

3.2 *ADVP*

The intensity of the backscattered acoustic signal over the depth obtained with the ADVP was recorded and used to determine the bed position and the top of the SFL. Over 32 successive pulses, the mean intensity (I_t) and the variance of the intensity (I_v) were computed. At rest, the bottom is estimated at the position of the maximum of I_t. When the sheet flow develops, it is assumed that the maximum intensity I_t is attained for a concentration corresponding to inter-particle distance equal to the Bragg wavelength. For the 0.2 mm sand considered in the present tests, this corresponds to a sediment concentration of 210 g/l, the upper limit of the SFL. Within the SFL, the concentration is very high and both the intensity variance and the mean intensity decrease in depth due to the strong damping of the acoustic wave. The immobile bed level is estimated from the level where a maximum of ($I_t - I_v$) is attained. This is illustrated in Figure 5, where vertical profiles of I_t, I_v and ($I_t - I_v$) are shown.

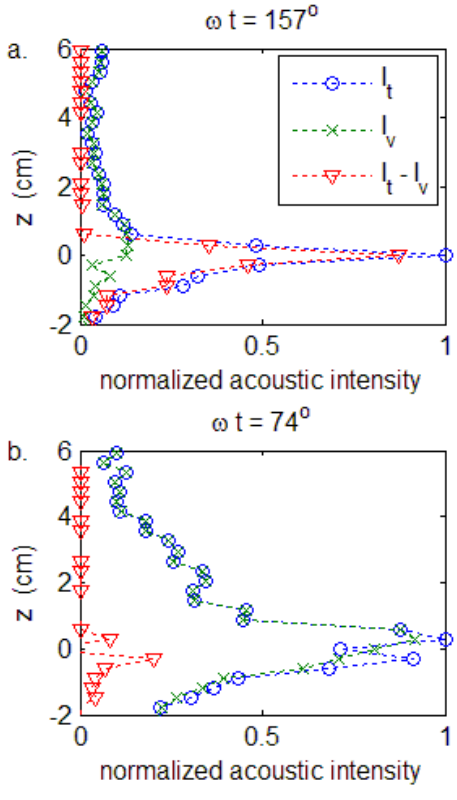

Figure 5. Vertical profiles of acoustic intensities for B2 condition at two different phases (see Figure 6c).

At flow reversal, the acoustic intensity (I_t) profile exhibits a narrow peak while its variance (I_v) is relatively small (Figure 5a). This indicates that most of the sediment is deposited and the bed interface is well defined. On the other hand, as the SFL develops, I_t and I_v are larger in the water column compared to the previous case (Figure 5b). The maximum in I_t is reached above the bed position at rest. Below the bed position at rest, the decay in I_v is stronger than the decay in I_t and a peak in ($I_t - I_v$) is clearly seen. This indicates that there is little sand grain movements at this level. This is interpreted as the bed position.

The mean intensity and the variance are estimated at 50 Hz. This is a discrete estimation of the SFL bounds at the location of the measurements (approximately each 3 mm). Low-pass filtering and phase-averaging the signal over more than 100 cycles leads to obtaining the curves plotted in Figure 6. It is thought that the high frequency fluctuations of the SFL bounds allow the estimation of their locations as mean quantities with an accuracy of the order of 1 mm.

3.3 *Video*

Observations of video recorded during the measurements, near the side glass of the LOWT, have enabled to estimate the erosion depth. In this case, d_e is the distance between the bed level at zero velocity after the crest positive velocity (when almost sediment has settled) and the lowest bed level observed during a wave cycle (at maximum velocity). This determination is not very accurate because it is difficult to distinguish the bed level at maximum velocities. The video observations were mainly used as a check of the other measurements presented.

4 RESULTS

Figure 6 shows the time variations of the lower and upper limits of the SFL computed from the CCM and ADVP data. The corresponding free stream velocity, measured by the EMF, and the acceleration time series for each hydraulic condition are shown in the upper part of each panel. Taking into account the very small scales involved and the errors associated in the determination of the upper and lower bounds of the SFL for both methods, an excellent overall agreement is found.

Both results illustrate the development of the SFL during the wave cycle: as the velocity increases from zero values, at each flow reversal, sediment particles are mobilized from the bed, thus causing local erosion associated with a deepening of the bed level and an increase in the erosion depth. These particles are entrained into the flow above the initial bed level (z=0) causing an increase of sediment concentration

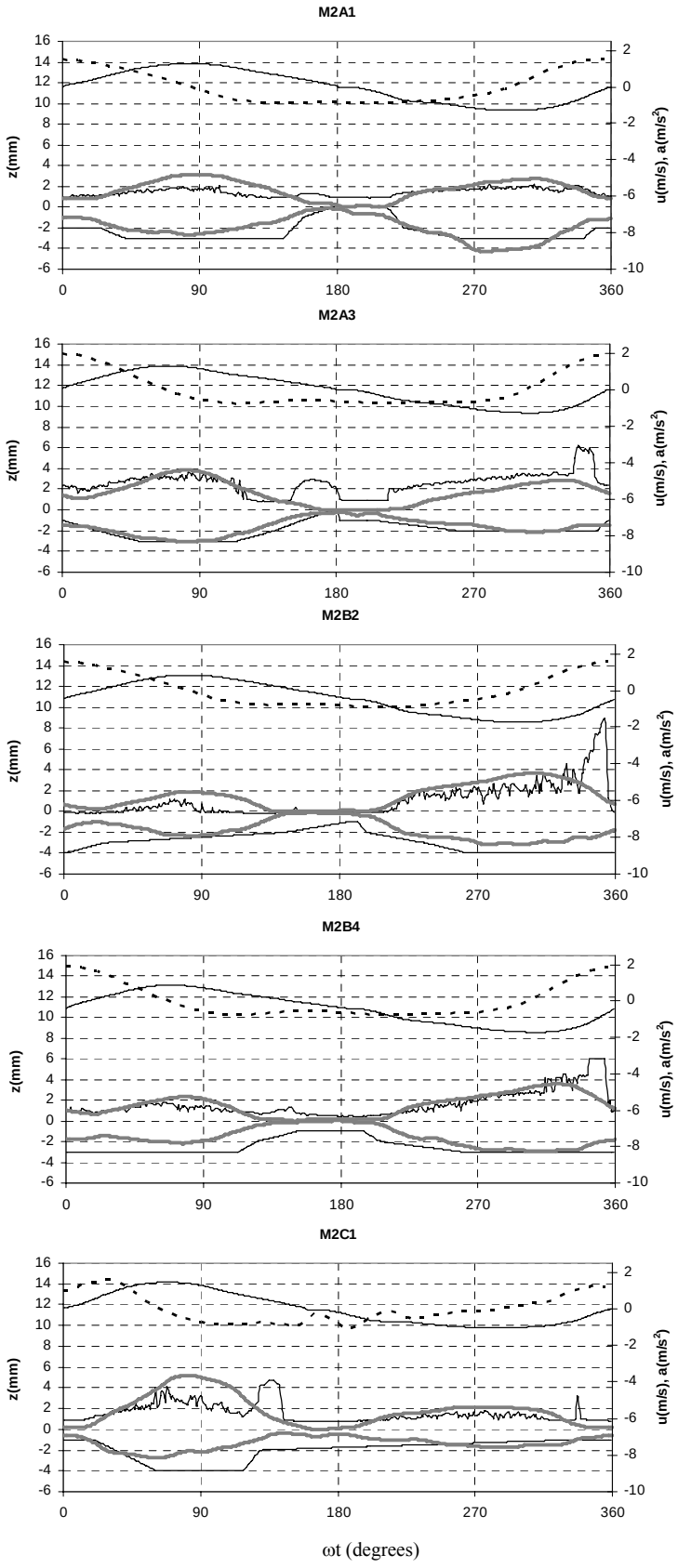

Figure 6. Lower and upper levels of the SFL computed from CCM (black solid lines) and ADVP (grey solid lines) for A1, A3, B2, B4 and C1 tests. The upper curves in each panel show the time series for the free-stream velocity (solid line) and acceleration (dashed line).

at those levels and, consequently, raising the top level of the SFL. When the magnitude of the velocity decreases, the processes that sustain the sediment particles either in the sheet flow or in the suspension layer tend to vanish, and sediment particles have a

tendency to settle down to the bed, causing a decrease in the SFL thickness. However, for all the test conditions, under the largest acceleration values, i.e., when the velocity changes rapidly from the offshore negative maximum to an onshore positive maximum, the SFL remains thicker than at the opposite on-offshore flow reversal where much smaller flow accelerations are found. This supports the existence of phase-lag effects between the sediment particles and the flow. This is confirmed by the video observations of the bed behaviour.

For the A3, B2, B4 and C1 conditions, the upper limit of the SFL computed from the CCM data show a sudden increase just before flow reversal. These maxima are connected to short duration concentration peaks measured by the CCM. Note that these peaks are more evident during the half cycles when more sediment has been entrained from the bed. According to other research works, the sediment peaks may be a signature of sediments settling into the bed (O'Donoghue and Wright, 2004) or due to shear instabilities in the wave boundary layer (for a discussion, see Ribberink *et al.*, 2008). As there is no evidence that the erosion depth increases at these moments (a feature also observed by O'Donoghue and Wright, 2004), this suggests that there is a vertical redistribution of the sediment already mobilized from the bed.

The major differences between the CCM and ADVP results consist in these reversal peaks that are not detected in the ADVP analysis. Overall, the values of d_e, d_t and δ_s attained at the maximum horizontal flow velocities are, respectively, in the range of −1.5 to −4 mm, 1 mm to 5 mm and 3.5 to 8 mm for both CCM and ADVP results. The values of the erosion depth retrieved from the video analysis are in the range of -1.2 to −1.5 mm: this is 45 to 70% lower than that computed from CCM and ADVP data. This can be explained because the video images were collected at the glass wall of the tunnel and are thus influenced by boundary effects.

The upper and lower bounds of the SFL at maximum velocity are well related to the physical forcing parameters. In test A3 (oscillatory flow with acceleration skewness) the erosion depth is larger under the crest than under the trough. This is in consonance with the numerical results of Hsu and Hanes (2004) and outcomes solely from the acceleration skewness, as the velocity skewness is zero in this test. This behaviour is also remarked at the upper level of the SFL and then consequently in δ_s. Note that test A1 does not show this tendency, neither for the CCM or ADVP results because the acceleration skewness is lower. It is also evident from Figure 6 that d_e, d_t and δ_s are proportional to the maximum flow velocity attained during the crest an trough. This can be achieved either by adding a mean current to the oscillatory flow, as in B2 and B4 tests, or increasing the onshore velocity in C1 test, resulting from an increase in the velocity skewness.

Note that the effect of the acceleration skewness described above is also perceptible in the combined wave–current tests: as the wave propagation direction and the current are opposite, an increase in the acceleration skewness (from B2 to B4 test) leads to an increase of the d_e and d_t (δ_s) during the crest and a decrease during the trough. This is particularly more evident in the CCM results.

5 CONCLUSIONS

New detailed measurements of time-dependent sediment concentrations and flow velocities were performed in acceleration- and velocity- skewed oscillatory flows. CCM and ADVP data were analysed to estimate the upper and lower SFL bounds along the oscillatory motion. Accordingly, the erosion depth and the SFL thickness were computed. The results obtained with both devices show a good agreement. It is shown that acoustic measurements could bring interesting observations in the SFL where the sediment concentration is very high.

The results show that the SFL thickness, δ_s, and the erosion depth, d_e, are nearly in phase with the free stream oscillatory flow, evidencing therefore a quick response of the bed. Furthermore, the acceleration and velocity skewness increase both d_e, mobilizing more sediment from the bed, and δ_s, at the wave crest.

Visual observations of the erosion depth from video recordings made at the tunnel glass wall underestimate the CCM and ADVP results.

The occurrence of short duration concentration peaks, just before the flow reversal, increase the upper level of the SFL. Some of these peaks are well marked (before the off-onshore flow reversal for A3, B2 and B4 tests) and seem related to the increasing flow acceleration. Also notice that at these phases, both CCM and ADVP results show that the erosion depth do not decay as faster to zero as in the on-offshore flow reversal, perhaps denoting the effect of larger accelerations in the erosion depth, as discussed by Hsu and Hanes (2004). This could justify a net transport in the wave direction for a saw-tooth wave, as measured in A3 test (Silva *et al.*, 2008), because the sediment that is mobilized during the trough is still available to be transported by the positive velocities in the next half-cycle. Furthermore, one can argue that the existence of a structured SFL at off-onshore flow reversal will enhance bed erosion as the velocity starts to increase at the crest.

The relation between the SFL structure, the bed shear stress and sediment fluxes is a subject of further analysis.

6 ACKNOWLEDGEMENTS

The experimental work was supported by the European Community's Sixth Framework Programme through the Integrated Infrastructure Initiative HYDRALAB III, Contract no. 022441(RII3).

The research was carried out within the frame of the research project PTDC/ECM/67411/2006 – BRISA, supported by FCT funding and the FCT/CNRS 2009 project cooperation.

Tiago Abreu has been supported by FCT through a PhD grant (SFRH/BD/41827/2007).

The authors acknowledge the fruitful discussions with many colleagues, especially Gerben Ruessink, Jan Ribberink and Eric Barthélemy.

7 REFERENCES

Abreu, T., Silva, P., and Sancho, F., 2008. Comparison of Sediment Transport Formulae Regarding Accelerated Skewed Waves. 31st International Conference on Coastal Engineering, ASCE, Hamburg, (in press).

Dohmen-Janssen, C.M., 1999. Grain size influence on sediment transport in oscillatory sheet flow: phase lags and mobile bed effects. PhD Thesis. Delft University of Technology.

Dohmen-Janssen, C.M. and Hanes, D.M. 2002. Sheet flow dynamics under monochromatic non-breaking waves. *J. Geophys. Res.*, 107(C10):1301–21.

Hsu, T.-J. and Hanes, D. M., 2004. Effects of wave shape on sheet flow sediment transport, *J. Geophys. Res.*, 109, C05025, doi:10.1029/2003JC002075.

Hurther, D., Michallet, H. and Gondran, X., 2007. Turbulent measurements in the surf zone suspension. *J. Coastal Res.*, SI50, 297 – 301.

McLean S.R., Ribberink, J.S., Dohmen-Janssen, C.M. and Hassan, W.N. 2001. Sand transport in oscillatory sheet flow with mean current. *J. Waterway Port Coast Ocean Eng.*, ASCE, 127(3):141–51.

Mignot, E., Barthélemy, E. and Hurther, D., 2009. Double-averaging analysis and local flow characterization of near-bed turbulence in gravel-bed channel flows. *J. Fluid Mech.*, 618, 279-303.

Myrhaug, D. and Holmedal, L.E., 2007. Mobile layer thickness in sheet flow beneath random waves. *Coast. Eng.* 54, 577–585.

O'Donoghue, T. and Wright, S., 2004. Concentrations in oscillatory sheet flow for well sorted and graded sands, *Coast. Eng.* 50, pp. 117–138.

Ribberink, J.S. and Al-Salem, A. 1994. Sediment transport in oscillatory boundary layers in cases of rippled bed and sheet flow. *J. Geophys. Res.*, 99 (C6):12707-12727.

Ribberink, J.S. and Al-Salem, A. 1995. Sheet flow and suspension in oscillatory boundary layers. *Coast. Eng.*, 25:205–225.

Ribberink, J. S., van der Werf, J. J., O'Donoghue, T. and Hassan, W. N. M., 2008. Sand motion induced by oscillatory flows: Sheet flow and vortex ripples, *Journal of Turbulence*, 9(20), 1-32.

Silva, P.A., Abreu, T., Freire, P., Kikkert, G., Michallet, H., O'Donoghue, T., Plecha, S., Ribberink, J., Ruessink, G., Sancho, F., Steenhauer, K., Temperville, A., Van der A., D. and Van der Werf, J., 2008. Sand transport induced by acceleration-skewed waves and currents – The TRANSKEW project. *PECS08 – Physics of Estuaries and Coastal Seas* (Liverpool, UK), 163-166.

Zala-Flores, N. and Sleath, J.F.A., 1998. Mobile layer in oscillatory sheet flow. *J. Geophys. Res.* 103 (C6), 12783–12793.